Journal of Scientific & Industrial Research
Vol. 71, May 2012, pp. 316-323

Modeling and optimization of a natural convection-based agricultural dryer

Rajesh Kumar and R V Ravikrishna*
Department of Mechanical Engineering, Indian Institute of Science (IISc), Bangalore 560 012

Received 24 March 2011; revised 08 March 2012; accepted 30 March 2012

This study presents development of a computational fluid dynamic (CFD) model to predict unsteady, two-dimensional temperature, moisture and velocity distributions inside a novel, biomass-fired, natural convection-type agricultural dryer. Results show that in initial stages of drying, when material surface is wet and moisture is easily available, moisture removal rate from surface depends upon the condition of drying air. Subsequently, material surface becomes dry and moisture removal rate is driven by diffusion of moisture from inside to the material surface. An optimum 9-tray configuration is found to be more efficient than for the same mass of material and volume of dryer. A new configuration of dryer, mainly to explore its potential to increasing uniformity in drying across all trays, is also analyzed. This configuration involves diverting a portion of hot air before it enters over the first tray and is supplied directly at an intermediate location in the dryer. Uniformity in drying across trays has increased for the kind of material simulated.

Keywords: Agricultural dryer, Computational fluid dynamic (CFD), Natural convection

Introduction

Direct sun drying takes a long time and may cause loss of colour, flavour, vitamins and contamination by dust and sand. Along with development of a number of agricultural dryers, models have also been developed to predict different parameters of such dryers. In a simulation model[1] for drying deep beds of grain typically consisting of a set of partial differential equations based on energy and mass balance in a bed element, drying coefficient depends both on external and internal resistance to moisture transfer. Arnaud & Fohr[2] used thin layer drying experiments to construct an equation for the rate of moisture loss of the bed as a function of temperature, humidity and velocity of air. Can[3] observed that drying takes place at the surface of drying material at a constant rate, and with decreasing drying rate. Simal & Rossello[4] proposed a heat and mass transfer (HMT) model for potato drying. Sharma *et al*[5] presented a mathematical model for drying of fruits and vegetables in a natural convection-type solar cabinet dryer. Wang & Chen[6,7] developed different HMT models and observed three basic mechanisms of water transfer occurring in the moist porous media (vapour diffusion, capillary flow and evaporation condensation). Sander *et al*[8] found that HMT coefficients are the functions of drying air characteristics and system geometry, whereas equilibrium moisture content is a function of air humidity and temperature only. Rigit & Low[9] conducted a computational fluid dynamic (CFD) study on a dryer design with a solar collector and chimney. Szafran & Kmiec[10] showed that CFD simulations predict mass transfer rate but underpredict heat transfer rate. Kaaya & Kyamuhangire[11] showed that drying maize grain with biomass dryer reduced drying time and greatly improved quality of grain during storage. Mohapatra & Mahanta[12] discussed development and evaluation of a natural convection grain dryer in drying performance of paddy. Looking into reviews of earlier studies, there is scant literature on biomass-fired natural convection-based dryers where drying takes place at the surface of drying material, and moreover, no computational analysis has been reported for such dryers. In this direction, Centre for Sustainable Technologies, IISc, Bangalore, has developed a fuel-efficient biomass-burning tray dryer[13] (Fig.1), where arrows show the direction of air movement, and dark spaces show the presence of drying material inside dryer.

Experimental Section

Modeling Methodology

Finite volume method for numerical solution of coupled conservation equations, and fully implicit method

*Author for correspondence
Tel: 91-80-22933226; Fax: 91-80-23600648
E-mail: ravikris@mecheng.iisc.ernet.in

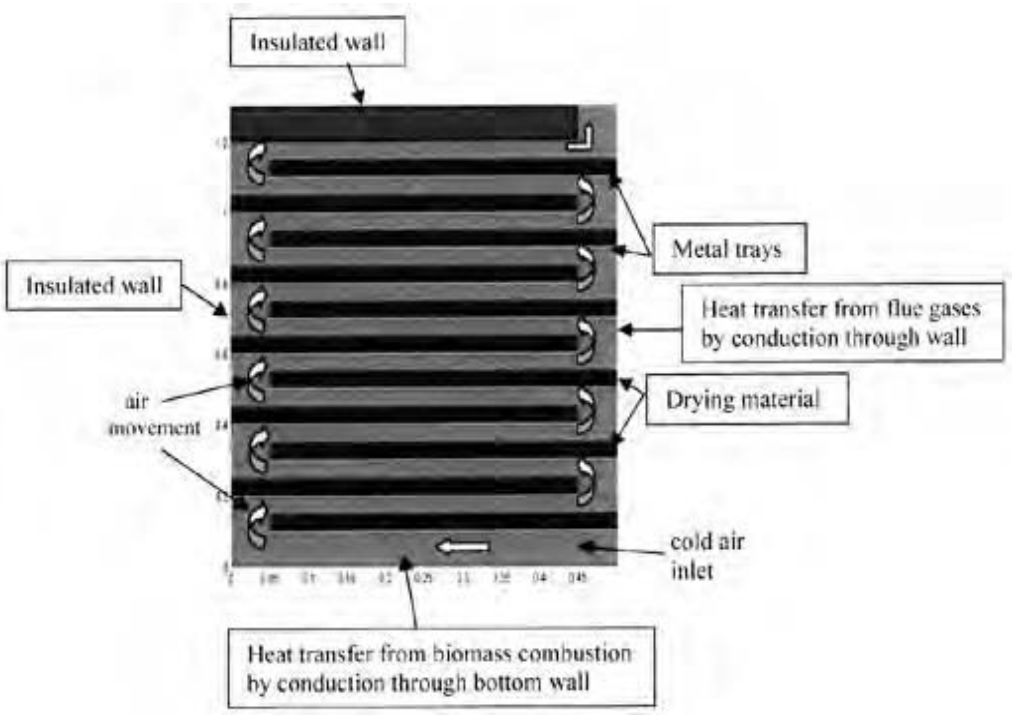

Fig. 1—Schematic of computational domain representing cross-section of dryer (dimensions in m)

for discretization of unsteady term were used. For diffusion term, central difference scheme was used. Power law scheme for discretization of convective term, and SIMPLER algorithm for flow field calculation were used. A very high value of viscosity is specified for solid part of dryer (metal trays and material). Top portion of dryer is extended so that flow becomes fully developed at dryer outlet. Efficiency (h) of drying process is the ratio of difference in moisture content of air at the exit and inlet to the difference in moisture content of air (saturated) at exhaust temperature and inlet moisture content, and is calculated as $h = (Y'_{exit} - Y'_{inlet})/(Y'_{sat}(T_{exit}) - Y'_{inlet})$, where Y' is specific humidity of air. Radiation heat transfer and heat loss from side walls is neglected. Temperature of bottom surface is assumed to be constant throughout the drying process. Porosity of material to be dried is neglected since most of the HMT occurs at the surface of material placed on tray. Variation along width of dryer is neglected rendering the problem two-dimensional. Continuity equation is given as

$$\frac{\partial (r u)}{\partial x} + \frac{\partial (r v)}{\partial y} = 0 \qquad ...(1)$$

where p is density of drying air and u, v are velocities of air along x and y-axis, respectively. The x-momentum equation for drying air is given as

$$\frac{\partial (r u)}{\partial t} + u\frac{\partial (r u)}{\partial x} + v\frac{\partial (r u)}{\partial y} = -\frac{\partial p}{\partial x} + m\left[\frac{\partial}{\partial x}\left(\frac{\partial u}{\partial x}\right) + \frac{\partial}{\partial y}\left(\frac{\partial u}{\partial y}\right)\right] \qquad ...(2)$$

where p is pressure, and m is viscosity of drying air. The y-momentum equation of drying air contains natural convection term, which produces buoyancy effect. This equation is given as

$$\frac{\partial (r v)}{\partial t} + u\frac{\partial (r v)}{\partial x} + v\frac{\partial (r v)}{\partial y} = -\frac{\partial p}{\partial y} + m\left[\frac{\partial}{\partial x}\left(\frac{\partial v}{\partial x}\right) + \frac{\partial}{\partial y}\left(\frac{\partial v}{\partial y}\right)\right] + r_t b\, g\,(T - T_{ref}) \qquad ...(3)$$

where r_t is density of air as a function of drying air temperature, b is thermal expansion coefficient of air, g is gravity, and T_{ref} is reference atmospheric temperature used for natural convection term. Energy equation for drying air consists of unsteady, convection and diffusion term and given as

$$\frac{\partial(r c_{pa}T)}{\partial t} + u\frac{\partial(r c_{pa}T)}{\partial x} + v\frac{\partial(r c_{pa}T)}{\partial y} = k_a\left[\frac{\partial}{\partial x}\left(\frac{\partial T}{\partial x}\right) + \frac{\partial}{\partial y}\left(\frac{\partial T}{\partial y}\right)\right] \quad ...(4)$$

where C_{pa} is specific heat capacity of air at constant pressure, and k_a is thermal conductivity of air.

Since there is no flow inside material and metal tray, energy equations inside material and metal plate contain only unsteady and diffusion terms, and given as

$$\frac{\partial(r_s c_{ps}T)}{\partial t} = k_s\left[\frac{\partial}{\partial x}\left(\frac{\partial T}{\partial x}\right) + \frac{\partial}{\partial y}\left(\frac{\partial T}{\partial y}\right)\right] \quad ...(5)$$

$$\frac{\partial(r_m c_{pm}T)}{\partial t} = k_m\left[\frac{\partial}{\partial x}\left(\frac{\partial T}{\partial x}\right) + \frac{\partial}{\partial y}\left(\frac{\partial T}{\partial y}\right)\right] \quad ...(6)$$

where r_s, C_{ps}, and k_s are density, specific heat capacity and thermal conductivity of drying material, respectively. Symbols r_m, C_{pm}, and k_m represent corresponding variables for metal.

When hot air flows over drying material, it heats the material by convection. At material surface, internal moisture evaporates and consumes latent heat of evaporation, leading to a decrease in material temperature. Energy equation at the interface on air-side is given as

$$\frac{\partial(r c_{pa}T)}{\partial t} + u\frac{\partial(r c_{pa}T)}{\partial x} + v\frac{\partial(r c_{pa}T)}{\partial y} = k_a\left[\frac{\partial}{\partial x}\left(\frac{\partial T}{\partial x}\right) + \frac{\partial}{\partial y}\left(\frac{\partial T}{\partial y}\right)\right] - a \times \frac{(T_a - T_s)}{L} \quad ...(7)$$

where a is convective heat transfer coefficient, T_a and T_s are absolute temperatures of air and material on either side of interface. Energy equation at interface on drying material side is given as

$$\frac{\partial(r_s c_{ps}T)}{\partial t} = k_s\left[\frac{\partial}{\partial x}\left(\frac{\partial T}{\partial x}\right) + \frac{\partial}{\partial y}\left(\frac{\partial T}{\partial y}\right)\right] - \frac{m''}{L} \times h_{fg} + a \times \frac{(T_a - T_s)}{L} \quad ...(8)$$

where m^2 is mass flux of moisture evaporated from material surface, L is length of tray, and h_{fg} is latent heat of vaporization of water.

Since air flows parallel to the bed of drying material and since flow is laminar in this zone [Reynolds number (Re) max. ~10^3], value of a is determined by using a correlation for convective heat transfer coefficient over a flat plate as $Nu_x = 0.332 Re_x^{1/2} Pr^{1/3}$, where Nu_x is local Nusselt number, Re_x is local Re and Pr is Prandtl number. Mass flux value is given as $m^2 = h_m r (X_s - X_\mu)$, where h_m is mass transfer coefficient, X_s is surface mass fraction of moisture, and X_μ is mass fraction of moisture far away from material surface. Here, h_m is calculated as $Sh_x = 0.332 Re_x^{1/2} Sc^{1/3}$, where Sh_x is local Sherwood number and Sc is Schmidt number. Species equation for drying air consists of unsteady, convection and diffusion terms, and is given as

$$\frac{\partial(rY)}{\partial t} + u\frac{\partial(rY)}{\partial x} + v\frac{\partial(rY)}{\partial y} = D_1 r\left[\frac{\partial}{\partial x}\left(\frac{\partial Y}{\partial x}\right) + \frac{\partial}{\partial y}\left(\frac{\partial Y}{\partial y}\right)\right] \quad ...(9)$$

where D_1 is binary diffusion coefficient and Y is mass fraction of water vapour in air.

Since moisture inside the material is transferred only by diffusion, species equation for drying material consists of only unsteady and diffusion terms. At the surface of drying material exposed to air, only water vapour was assumed to be present in control volume. So, density at the surface control volume is taken as density of water vapour at that temperature. Equation used to predict moisture concentration in the material except at the surface is given as

$$\frac{\partial(r_s X)}{\partial t} = D_2 r_s\left[\frac{\partial}{\partial x}\left(\frac{\partial X}{\partial x}\right) + \frac{\partial}{\partial y}\left(\frac{\partial X}{\partial y}\right)\right] \quad ...(10)$$

where D_2 is diffusivity of moisture inside the material. For all control volumes at material surface, equation used is as

$$\frac{\partial(r_v X)}{\partial t} = D_2 r_v\left[\frac{\partial}{\partial x}\left(\frac{\partial X}{\partial x}\right) + \frac{\partial}{\partial y}\left(\frac{\partial X}{\partial y}\right)\right] \quad ...(11)$$

where r_s and r_v are density of drying material and water vapour, respectively, and X is mass fraction of moisture in the material. Boundary conditions adopted include no-slip condition at the walls, fully developed flow at the outlet, constant temperature at the bottom surface, insulated left and top surfaces, specified moisture content for entering air and zero moisture content gradient at the walls.

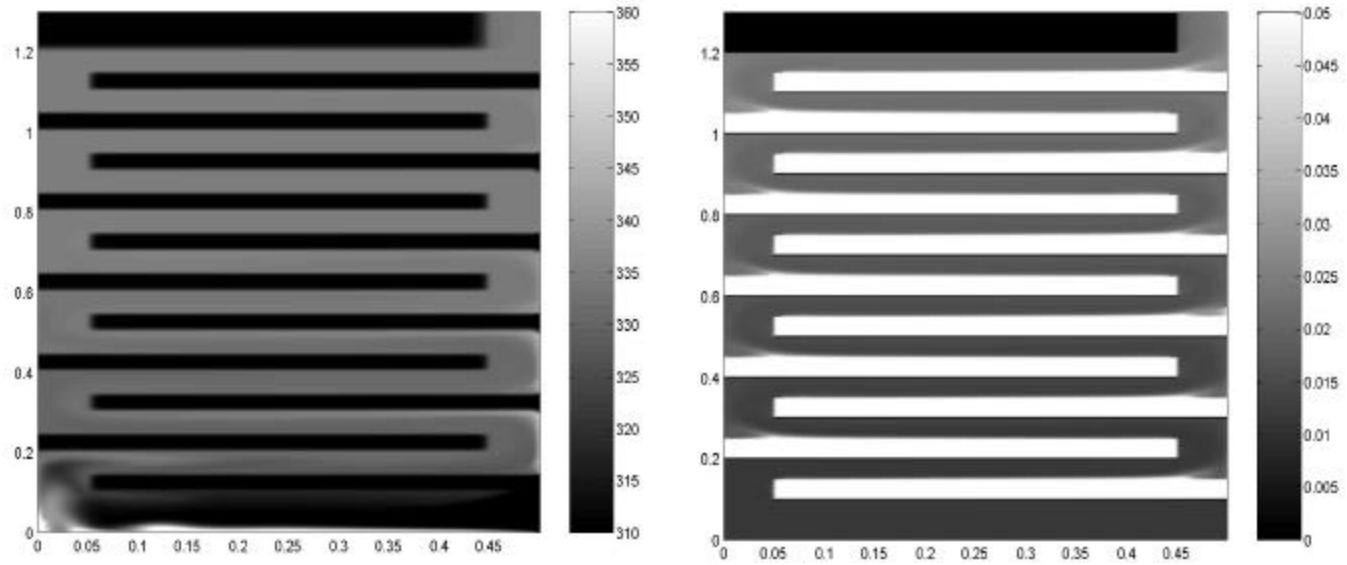

a) b)

Fig. 2—For dryer with 11 trays at 10 min after start of drying: a) temperature distribution (K); and b) water vapour mass fraction contours (physical dimensions on x and y axes are in m)

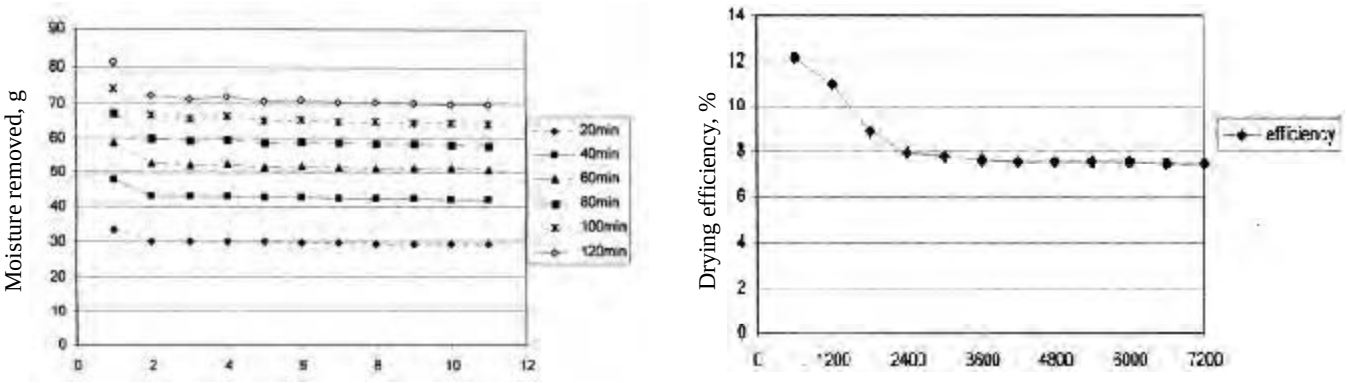

a) b)

Fig. 3—Variation during drying (2 h) of apple in: a) moisture removed at intervals of 20 min; and b) drying efficiency

Results and Discussion

Simulation was first performed for geometry of existing dryer configuration and using apple as drying material with properties as reported[8,14]. Variation of thermal conductivity of drying material as a function of its moisture content was used as reported[15]. Temperature of bottom duct surface was taken as 410 K. Numerical values used for simulation are given as: specific heat capacity of apple & banana; 3600 & 3350 J/kg-K; specific heat capacity of air & steel tray, 1009 & 480 J/kg-K; thermal conductivity of air & steel tray, 0.0285 & 17.3 w/m-K; density of apple & banana, 840 & 980 kg/m^3; density of steel tray, 7900 kg/m^3; initial mass fraction of water in apple & banana, 0.75 & 0.757; diffusivity of water vapour in air, 2. 610^{-5} m^2/s; diffusivity of water in apple & banana, 2.1610^{-10} & 2.9610^{-10} m^2/s; and viscosity of air, 2.0510^{-5} kg/m-s. For model validation purposes, total air flow rate under natural convection for biomass-fired dryer was measured in terms of air velocity at the exit. Measured value (1.8 cm/s) compared very well with predicted value (1.6 cm/s).Simulation was performed for 2 h. Since heat is transferred by conduction from bottom wall, temperatures closest to bottom wall were highest (Fig. 2), and there was mixing between this hot fluid and colder air coming in from the inlet. Similarly, since heat is conducted from right-side wall also, temperatures near this wall were observed to be higher. Moisture removal rate decreases with increase in time (Fig. 3a). When surface moisture level reaches an equilibrium, moisture removal rate depends upon

Table 1—Description of cases simulated

Case No.	No. of trays	Length/depth of material, cm	Description of problem
1	11	45/5	Original dryer configuration using apple
2	11	45/5	Original dryer configuration using banana
3	11	56/4	Case 1 with change in depth of material on tray
4	11	35/6.4	Case 1 with change in depth of material on tray
5	11	75/3	Case 1 with change in depth of material on tray
6	9	55/5	9 trays with different depth of material on tray
7	9	68.75/4	9 trays with different depth of material on tray
8	9	46/6	9 trays with different depth of material on tray
9	9	92/3	9 trays with different depth of material on tray
10	7	47.5/7.5	7 trays with different depth of material on tray
11	7	59/6	7 trays with different depth of material on tray
12	7	88/4	7 trays with different depth of material on tray
13	7	118/3	7 trays with different depth of material on tray
14	11	45/5	Case 1 with a portion of hot air supplied at 7th tray
15	9	92/3	Case 9 with a portion of hot air supplied at 3rd tray
16	9	92/3	Case 9 with a portion of hot air supplied at 5th tray
17	9	92/3	Case 9 with a portion of hot air supplied at 7th tray

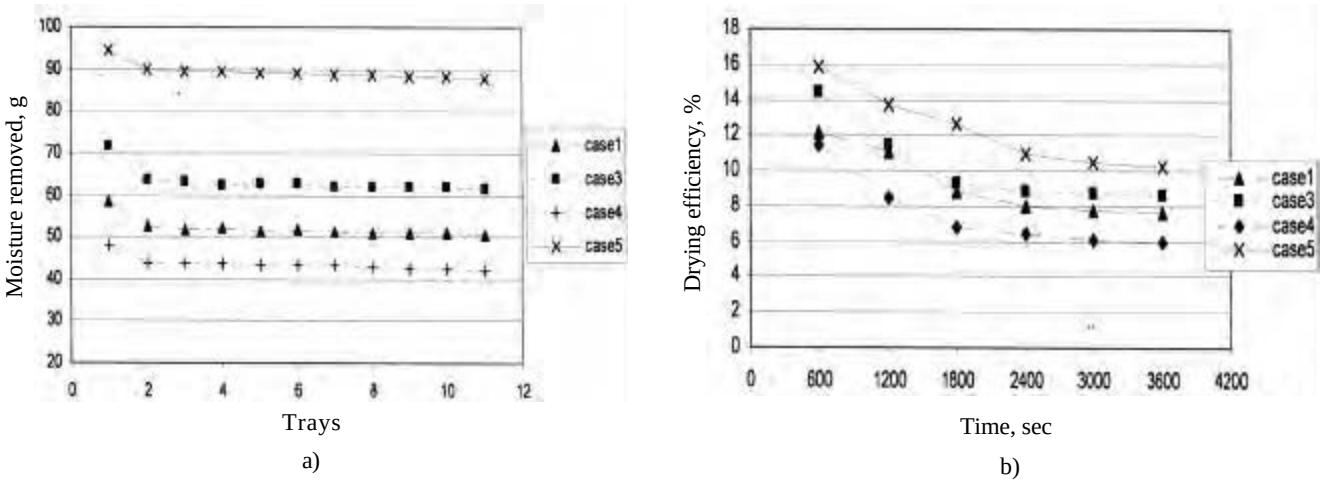

a) b)

Fig. 4—Variation for dryer with 11 trays and different bed depths of material in: a) moisture removed; and b) efficiency

internal diffusivity of moisture inside the material. Also, efficiency is observed higher in initial stage of drying and decreases as time progresses (Fig. 3b), mainly because of increased availability of moisture at the surface in initial stage of drying.

Simulations were performed for different cases, in which depth of drying material on the tray was varied (Table 1). It was observed that decrease in material depth increases moisture removal rate as well as efficiency of drying (Fig. 4). This is because in a tray-type dryer, evaporation mainly occurs at bed surface, and spreading the bed increases surface area exposed to the drying air, thereby increasing rate of moisture removal. For materials of small dimension, such as cardamom, it can be thinly spread, and hence this type of dryer will be more effective. In present simulation, minimum depth of material was taken as 3 cm. Initially, efficiency is 12-16%, but then it reduces to 6-11% after 40 min of drying.Simulations were performed with 9 and 7 trays for different material bed depths. It was observed that for a particular set of trays, moisture removal rate and efficiency increase with decrease in material depth on

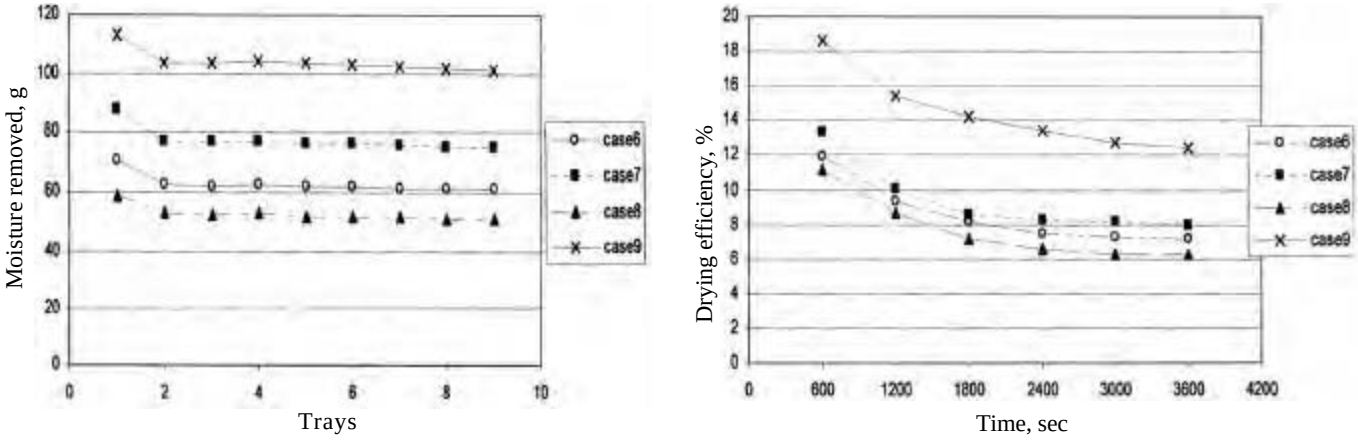

a) b)

Fig. 5—Variation for dryer with 9 trays and different bed depths of material in: a) moisture removed; and b) efficiency

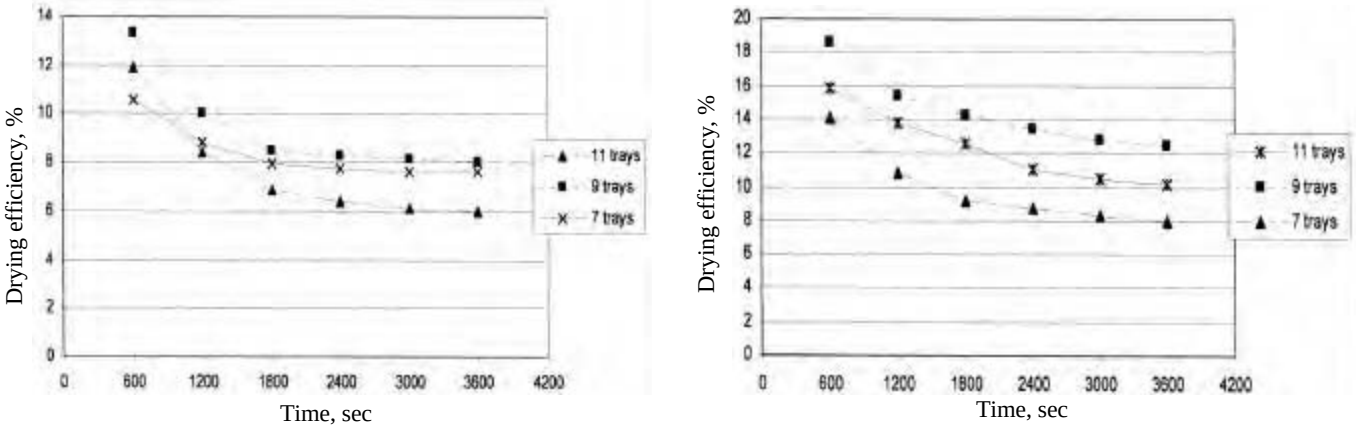

a) b)

Fig. 6—Variation of efficiency in 1 h of drying for dryer with different number of trays : a) 4-cm bed depth of material; and b) 3-cm bed depth of material

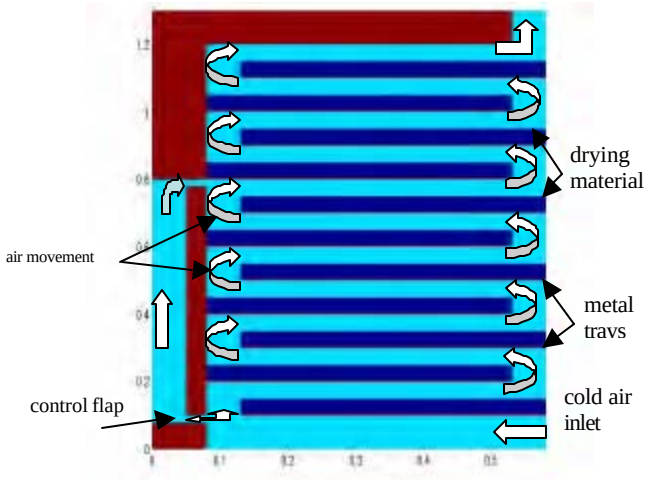

Fig. 7—Schematic of the cross-section of dryer with split-air-flow geometry

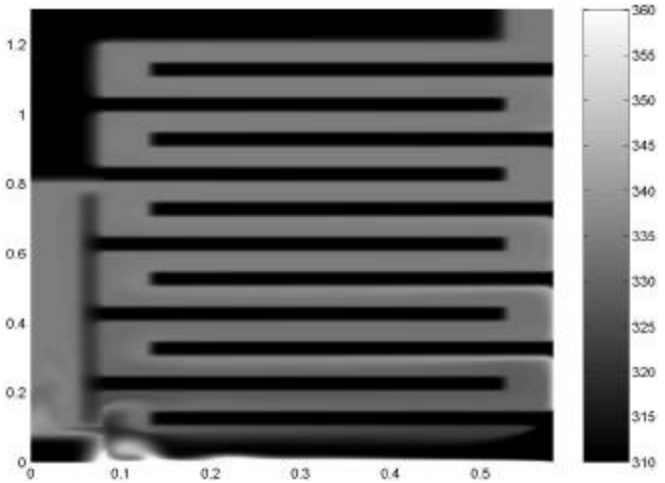

Fig. 8—Temperature distribution for dryer with split-air-flow geometry and 11 trays at 10 min after start of drying

tray (Fig. 5). This is because decrease in material depth on tray increases surface area of material exposed to drying air, thereby increasing rate of moisture removal. A 9 tray configuration with 3-cm bed depth of material shows

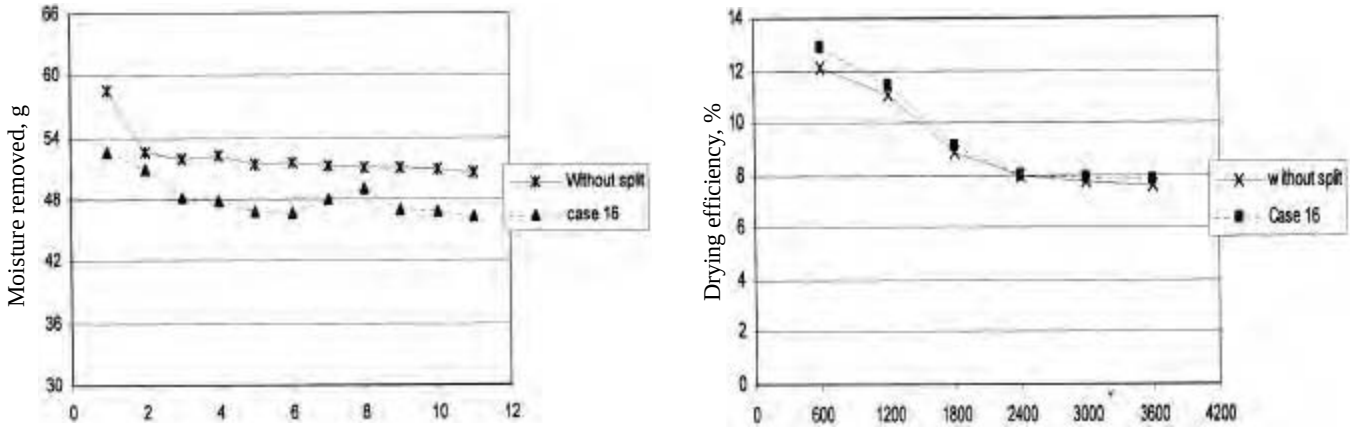

Fig. 9—Comparison between original dryer (with 11 trays) and dryer with split-air-flow geometry for: a) moisture removed; and b) efficiency

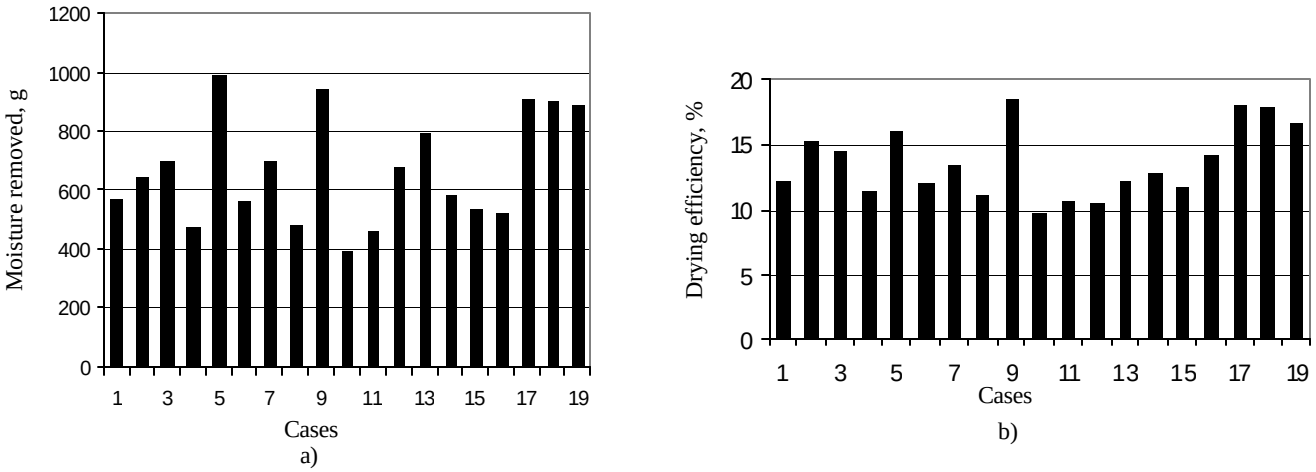

Fig. 10—For all cases: a) total moisture removed; and b) maximum efficiency

improved performance in terms of drying efficiency, as compared to other cases (Fig. 6).

A new geometry of dryer (Fig. 7) is proposed to increase uniformity in drying across all trays. In this configuration, provision is made to divert a portion of hot air from the bottom and supply it directly at an intermediate location in dryer, in order to provide hot air with less humidity to upper trays so that air has more capacity to drag moisture from upper trays and increases uniformity of drying. The cold atmospheric air after passage over the bottom duct gets heated and a portion is diverted before it enters over the first tray by providing a small opening at the left end. This portion of hot air is supplied at 7th tray through a duct provided at the left end and it mixes with humid air circulating over all trays. For this split-air-flow configuration, length of opening is 2 cm, and 36% by mass of hot air is directly supplied to 7th tray. The plot (Fig. 8) shows that temperature at the exit of dryer is higher compared to that in the original geometry of dryer. Comparisons of moisture variation (Fig. 9a) and efficiency (Fig. 9b) are shown for dryer with 11 trays and 5 cm bed thickness with and without split geometry. It is observed (Fig. 9a) that total moisture removed in split-air-flow geometry case is decreased, but variation in moisture removed from first to eleventh trays has also reduced, may be due to flow rate of drying air has decreased over the first seven trays in the case of split-air-flow geometry. Also, moisture removed from 8^{th} tray is more than that from 7^{th} tray, when fresh air is supplied at the beginning of 7^{th} tray, due to improper mixing of fresh air with moist air in initial stage as observed in the mass fraction contour plot. Efficiency is observed to increase for new configuration during initial stage of drying, but almost same as time proceeds (Fig. 9b),

because in initial stage, material surface is wet, but as time progresses, drying depends upon internal diffusivity of the material.

It was observed that amount of total moisture removed (Fig. 10a) was maximum for case 5 (dryer with 11 trays and 3 cm bed depth), while efficiency (Fig. 10b) was maximum for case 9 (dryer with 9 trays and 3 cm bed depth); the last three cases correspond to split-air-flow geometry configuration with 9 trays. However, efficiency and moisture removed for these three cases are less than those of case 9 with original geometry, mainly due to decreased air-flow rate over the first few trays. For a material with very high internal moisture diffusivity, split-air-flow geometry can become more efficient. However, for materials with similar diffusivity as apple and a bed depth of 3 cm, case 9 (original dryer configuration with 9 trays) is the optimum configuration.

Conclusions

In initial stages of drying, when surface of material is wet and moisture is easily available, moisture removal rate from the surface depends upon the condition of drying air. Subsequently, material surface becomes dry and moisture removal rate is driven by diffusion of moisture from inside to the surface of material. Number of trays in dryer was found to be an important parameter affecting drying efficiency. An optimum 9 tray dryer configuration has been identified with a 50% improvement in drying efficiency. Simulations for a new split-air-flow configuration of dryer show that moisture removal rate is slightly decreased compared to that of the original configuration. However, uniformity in drying across trays was observed to have improved with this configuration. Also, split-air-flow configuration of dryer shows potential for improved drying efficiency for materials with very high internal moisture diffusivity.

References

1 Milojevic D Z & Stefanovic M S, Convective drying of thin and deep beds of grain, *Chem Engg Commun*, **13** (1982) 261-269.

2 Arnaud G & Fohr J P, Slow drying simulation in thick layers of granular products, *Int J Heat Mass Transfer*, **31** (1988) 2517-2526.

3 Can A, Drying kinetics of pumpkin seed, *Int J Energy Res*, **24** (2002) 965-975.

4 Simal S & Rossello C, Heat and mass transfer model for potato drying, *Chem Engg Sci*, **49** (1994) 3739-3744.

5 Sharma V K, Sharma S & Garg H P, Mathematical modeling and experimental evaluation of a natural convection type solar cabinet dryer, *Energy Convers Manage*, **43** (1991) 65-73.

6 Wang Z. H & Chen G, Heat and mass transfer during low intensity convection drying, *Chem Engg Sci*, **54** (1999) 3899-3908.

7 Wang Z H & Chen G, Heat and mass transfer in fixed bed drying, *Chem Engg Sci*, **54** (1999) 4233-4243.

8 Sander A, Kardum J P & Skansi D, Transport properties in drying of solids, *Chem Biochem Engg Q*, **15** (2001) 131-137.

9 Rigit A R H & Low P T K, Heat and mass transfer in a solar dryer with biomass backup burner, *World Acad Sci, Engg Technol*, **62** (2010) 115-118.

10 Szafran R G & Kmiec A, CFD modelng of heat and mass transfer in a spouted bed dryer, *Ind Engg Chem Res*, **43** (2004) 1113-1124.

11 Kaaya A N & Kyamuhangire W, Drying maize using biomass-heated natural convection dryer improves grain quality during storage, *J Appl Sci*, **10** (2010) 967-974.

12 Mohapatra S S & Mahanta P, Performance evaluation of quality drying in a natural convection dryer, *Appl Mech Mater*, (2011) 110-116, 2094.

13 Sreekumar, *Internal Report* (Centre for Sustainable Technologies, Indian Institute of Science, Bangalore) 2002.

14 Dewitt D P & Incropera F P, *Fundamentals of Heat and Mass Transfer*, **4th edn** (John Wiley & sons, New York) 1990.

15 Srinivasan K & Wijeysundera N E, Heat and moisture transport in wet cork slabs under temperature gradients, *Build Environ*, **36** (2001) 53-57.